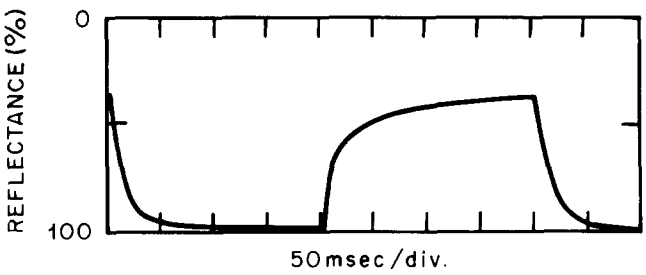

FIG. 3. Transmission modulation for a SIROF deposited on Ta for a square wave voltage drive of 0–1 V versus SCE. The zero for the vertical axis is indicated, and transmitted light intensity increases downward. The area (geometric) exposed to the electrolyte is ≈ 1 mm^2.

shown in Fig. 3. Since the yellow state is more highly reflecting at 633 nm than is the blue state, an increase in anodic voltage increases the reflected light as shown in Fig. 3, rather than decreasing it as is observed for AIROFs on iridium substrates.

SIROFs also are extremely stable. The response shown in Fig. 3 was found to be unchanged after $\approx 10^6$ cycles of 1-V amplitude and a 0.2-sec period. Although not completely understood, the various colors observed for SIROFs deposited on tantalum could result in part from interference effects due to an interfacial tantalum oxide film, or from incorporation of tantalum into the SIROF. However, Auger measurements showed no evidence for any Ta at or near the SIROF surface. We have also prepared an all-solid-state device by depositing SIROFs on Nafion, opacified as described in Ref. 6. The properties of these devices will be described in detail elsewhere.

The exact role of the water in the sputtering atmosphere is still uncertain, since SIROFs grown subsequently without any deliberate humidification exhibit an electrochromic effect. We are presently studying the effects of H_2O and O_2 partial presures upon contrast, speed, and stability of the resulting films.

In conclusion, we have shown that reactively sputtered iridium oxide films (SIROFs) have the fast kinetics and good stability previously reported for AIROFs. They are, therefore, a very promising material for practical electrochromic display devices. Moreover, SIROFs deposited on various metal substrates manifest a variety of colors which add a new dimension to the range of potential applications for iridium oxide displays.

We are grateful to A.M. Glass and D.H. Olson for the use of their sputtering apparatus, and to E. Hu and P. Grabbe for performing the Auger measurements.

[1]S. Gottesfeld, J.D.E. McIntyre, G. Beni, and J.L. Shay, Appl. Phys. Lett. **33**, 208 (1978).
[2]G. Beni and J.L. Shay, Appl. Phys. Lett. **33**, 567 (1978).
[3]J.L. Shay, G. Beni, and L.M. Schiavone, Appl. Phys. Lett. **33**, 942 (1978).
[4]G. Beni and J.L. Shay, Proc. of Int. Conf. on Fast Ion Transport in Solids, Lake Geneva, Wisc., 1979 (unpublished).
[5]W.C. Dautremont-Smith, G. Beni, L.M. Schiavone, and J.L. Shay, Proc. of Int. Conf. on Fast Ion Transport in Solids, Lake Geneva, Wisc., 1979 (unpublished).
[6]W.C. Dautremont-Smith, G. Beni, L.M. Schiavone, and J.L. Shay, Appl. Phys. Lett. **35**, 565 (1979).
[7]S. Gottesfeld and J.D. E. McIntyre, J. Electrochem. Soc. **126**, 742 (1979).

Depth dependence of atomic mixing by ion beams

B. Y. Tsaur, S. Matteson, G. Chapman,[a] Z. L. Liau,[b] and M-A. Nicolet
California Institute of Technology, Pasadena, California 91125

(Received 6 July 1979; accepted for publication 4 September 1979)

Ion backscattering spectrometry has been used to investigate the depth dependence of atomic mixing induced by ion beams. Samples consisting of a thin Pt (or Si) marker a few tens of angstroms thick buried at different depths in a deposited Si (or Pt) layer were bombarded with Xe^+ of 300 keV at 2×10^{16} cm^{-2} dose and Ar^+ of 150 keV at 5×10^{15}cm^{-2} dose. Significant spreading of the marker was observed as a result of ion irradiation. The amount of spreading was measured as a function of depth of the marker, which was then compared with the deposited energy distribution. Measurements of this kind promise new insight into the nature of the interaction between ion beams and solids.

PACS numbers: 25.70. − z, 29.70.Gn, 61.70.Wp, 64.75. + g

When energetic ions penetrate into a solid, they suffer a series of energy-degrading collisions with the target atoms and thereby induce atomic displacements. As a consequence, an implantation of many incident ions produces a disordered region of a thickness which is commensurate with the range of the ion. The spatial distribution of the disorder has been studied extensively for ions penetrating uniform media.[1,2] Only a few experiments have been reported on the phenomenon of ion-beam-induced intermixing that occurs when an ion traverses a layered sample. Lee, Hart, and Marsh[3,4] implanted ions through Al films on Si and observed

[a]Permanent Address: School of Applied Sciences, Riverina College of Advanced Education, Wagga Wagga, NSW, Australia.
[b]Permanent Address: Lincoln Laboratory, Massachusetts Institute of Technology, Lexington, Massachusetts 02173.

 0003-6951/79/220825-04$00.50

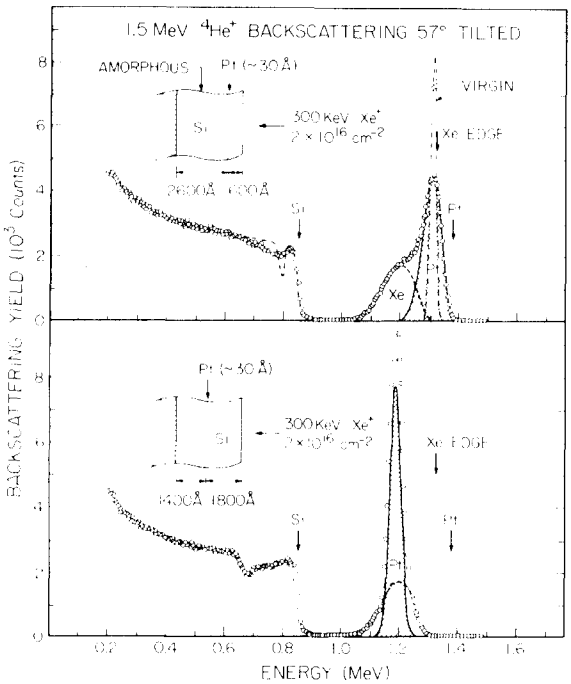

FIG. 1. Backscattering spectra of two Si samples, each buried with a thin Pt marker, implanted with 300-keV Xe$^+$ to a dose of 2×10^{16} cm^{-2}. Significant differences in the amount of spreading (due to ion bombardment) are shown for Pt markers buried at different depths. The samples were tilted 57° in the backscattering measurements to improve the depth resolution. The spectrum of the "virgin" specimen, i.e., unbombarded specimen, is also given for comparison.

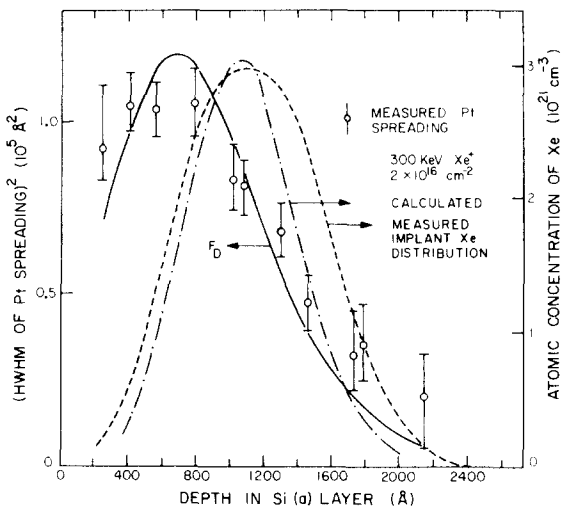

FIG. 2. Depth dependence of ion-induced Pt marker spreading calculated by using Eq. (1). Each open circle represents a Pt marker buried at different depths. The solid curve is the result of calculations using Eq. (2), where $(\mathrm{HWHM})^2 \propto F_D$, the deposited elastic energy distribution. Dash curve is the measured range distribution of Xe ions. Dash-dot curve is the range distribution predicted by the Winterbon calculation.

an enhanced interaction between film and substrate upon subsequent annealing. Similar experiments were reported also for the compound-forming metal films, Pd[5,6], Pt[7,8], Ni[8], Nb[9], and Ti[10] on Si substrates. The clarification of the processes responsible for the ion-beam-induced intermixing requires detailed experimental information on the process at a microscopic level. The present investigation demonstrates a promising experimental method which offers such insight by revealing the evolution of ion-induced intermixing with dose at a specific location with a marker.

Thin-film samples with a ~30-Å-thick Pt marker buried in an amorphous Si layer were prepared by sequential vacuum deposition of Si and Pt onto clean silicon substrates. The location of the Pt marker ranged from 200 to 2000 Å below the sample surface. The total thickness of the amorphous Si layer was about 3200 Å (see insert in Fig. 1). The electron-gun evaporation was performed in an oil-free vacuum system at an average deposition rate of ~5 Å/sec in a vacuum better than 4×10^{-7} Torr. Another set of samples, each with a ~60-Å Si marker buried in a Pt layer ~960 Å thick, was also prepared by the same procedure. The samples were implanted at room temperature at average current densities of 1 μA/cm^2 with 300-keV Xe$^+$ to 2×10^{16} cm^{-2} and with 150-keV Ar$^+$ to 0.5×10^{16} cm^{-2}. Thermally conductive adhesive avoided heating of the samples by the ion bombardment. The depth distributions of the implanted ion and the markers were measured by 1.5-MeV ^{4}He ion backscattering.

The depth resolution was estimated to be approximately 200 Å near the surface for Pt in Si and approximately 70 Å near the surface for Si in Pt. The uncertainty introduced by this limited depth resolution of the ion backscattering spectrometry is indicated in Figs. 2 and 3 by the vertical error bars.

Figure 1 shows the backscattering spectra of two samples, each with a Pt marker buried at different depth, implanted with 300-keV Xe ions to a dose of 2×10^{16} cm^{-2}. The projected range of the Xe is about 1100 Å, so that the average Xe ions penetrated about half-way through the Si layer. The signal appearing in the high-energy part is that of the Pt marker superimposed to that of the implanted Xe as measured from a Xe-implanted sample without Pt marker. Since the amount of Pt is small, the Xe ion distribution was assumed to be unaffected by the presence of the marker. The

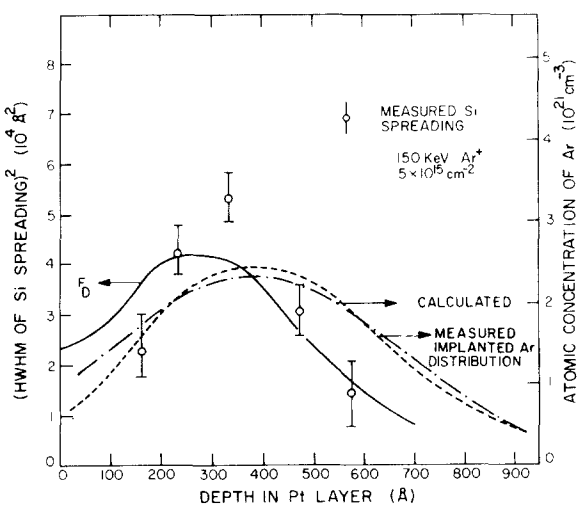

FIG. 3. Depth dependence of ion-induced Si marker spreading calculated by using Eq. (1). Each open circle represents a Si marker buried at different depths. The solid curve is the result of calculations using Eq. (2), where $(\mathrm{HWHM})^2 \propto F_D$, the deposited elastic energy distribution. Measured Ar ions distribution is shown by the dash curve. Dash-dot curve is the range distribution according to the Winterbon calculation.

spectra clearly reveal the spreading of the marker as a result of the Xe implantation. The spectra also show that there are significant differences in the amount of Pt spreading for markers that are located at different depths.

The energy vsariance of the marker spreading caused by the implantation was derived according to

$$(\text{HWHM of marker spreading})^2 = \epsilon^2 - \sigma^2, \qquad (1)$$

where σ and ϵ are HWHM (half-width of half-maximum) of the Pt signal measured before and after ion implantation. The variance is chosen to characterize the marker spreading because we have noted that this quantity increases roughly linearly with the ion dose ϕ. Figure 2 shows the energy variance of the Pt marker spreading after Xe bombardment as a function of depth from the surface. Each open circle represents a marker buried at a different depth. For comparison the dashed curve shows the implanted Xe profile derived from the backscattering spectrum of the reference sample without a Pt marker.

Similar results have also been obtained for Pt films with a buried Si marker and implanted with 150-keV Ar^+ to a dose of $0.5\times10^{16}\,\text{cm}^{-2}$. Since the backscattering cross section of Ar for He is small, the implanted Ar distribution (dashed line in Fig. 3) was measured from the spectrum of a sample without Si marker and implanted to a threefold dose of $1.5\times10^{16}\,\text{cm}^{-2}$.

Our results establish four facts: (i) Ion backscattering spectrometry in combination with very thin layers of atoms differing significantly in their mass from that of the target can reveal the intermixing of atoms induced by an ion beam penetrating the target, (ii) the amount of intermixing observed after ion irradiation varies with depth, (iii) the amount of intermixing extends over a depth commensurate with the range of the ion, but the depth profiles of the mixing and of the ion range differ, and (iv) the variance of the marker spread increases approximately linearly with the ion dose.

We believe that this marker type of an experiment provides a more direct insight into the processes controlling the interaction between an energetic particle and a solid target than experiments investigating the modifications that occur at interfaces as a result of particle irradiation, such as sputtering of compound layers (solid-vacuum interface)[11] or the intermixing of a thin film with the substrate (substrate-film interface).[8,9] In fact, our observation that the amount of intermixing varies with depth means that a correct interpretation of those experiments requires a detailed knowledge of the beam-solid interaction over the whole range of depths covered by the impinging ion. That type of information is provided by experiments with very thin markers as presently described.

To properly interpret the results of Figs. 2 and 3 in terms of the basic atomistic processes at hand requires circumspection. First, one has to assume that our results are independent of the way in which the samples were prepared. Light reactive elements (H, C, N, O) could easily be incorporated in considerable amounts at interfaces without being detected by backscattering spectrometry. Second, the spreading must, in general, be a function of the pair of elements selected for the target and the marker. This choice can alter the outcome in several ways: by virtue of (i) their respective masses, (ii) their chemical affinity, and (iii) their physical characteristics (i.e., single-crystalline versus amorphous film and/or marker). Third, the idea of a very thin "marker" invoked so far implies that the result should be independent of the amount of material used for the marker.

These critical arguments notwithstanding, it is interesting to compare our results with models proposed by Haff and Switkowski[12] and by Andersen,[13] which consider mixing to be the result of cumulative random-walk-like displacements. An appropriate modification of Andersen's model to get the depth dependence of mixing leads to the prediction that[14]

$$Dt = \tfrac{1}{6}(0.42)(F_D/N_0)\phi\,(\langle r^2\rangle/E_d), \qquad (2)$$

where $Dt \equiv (\text{half-width})^2/4\ \ln 2$, F_D is the distribution of energy causing atomic displacement, i.e., deposited elastic energy, ϕ is the fluence, $\langle r^2\rangle$ is the mean square displacement of an atom in the collision cascade, and E_d is the effective displacement energy. There is qualitative agreement between our results and Eq. (2). The half-width increases as $\phi^{1/2}$. In both Figs. 2 and 3, the deposited elastic energy distribution, predicted by the Winterbon calculation,[15] is least-squares normalized to the observed mixing. The shape and position of the distributions agree fairly well.

With the present state of the evidence we cannot attribute significance to the discrepancy between the normalized theoretical distribution and the experimentally measured spreading of the markers shown in Figs. 2 and 3. This conclusion is based upon the observed and theoretical *range* distributions rather than the F_D distribution. In the case of Pt in Si the theoretical range distribution is narrower than the observed, while in the case of Si in Pt the theoretical range distribution is wider than the observed. The relationship between the respective theoretical F_D distributions and the measured spreading of the markers is similar to that of the corresponding theoretical and experimental range distributions. Although a power law relation of $(\text{HWHM})^2 \propto F_D^{0.6}$ for Pt in Si and $(\text{HWHM})^2 \propto F_D^{1.5}$ for Si in Pt yields a closer apparent agreement between the calculated F_D distribution and the observed mixing, we believe that such power law relations are spurious, and if the error in the width of the theoretical range distributions were reduced, a closer agreement between $(\text{HWHM})^2 \propto F_D$ and the observed spreading would occur also. Therefore, within the accuracy of the range theory, the spread of the markers $(\text{HWHM})^2$ is proportional to F_D, the deposited energy in elastic collisions.

Moreover, Eq. (2) predicts only symmetric spreading of the marker. Indeed, this was observed. All markers spread symmetrically. Thus, a qualitative agreement is obtained between experiment and Eq. (2). In order to further substantiate the validity of the comparison of the mixing and calculated damage distributions, the predicted and observed range distributions are also compared. They agree to approximately the same extent as the mixing distributions do.

The least-squares fit of Eq. (2) to the data (using $\langle r^2\rangle/E_d$ as the fitting parameter) gives a value for $\langle r^2\rangle/E_d$ of 70 Å^2/eV for Xe incident on Si (with Pt marker) and 200 Å^2/eV for Ar incident on Pt (with Si marker). This indicates

that $\langle r^2 \rangle^{1/2}$ should be approximately 30 Å for Si (with $E_d \simeq 13$ eV) and 85 Å for Pt (with $E_d \simeq 36$ eV).[13] These values should be contrasted with the corresponding values of 6 Å suggested by Andersen[13] for $\langle r^2 \rangle^{1/2}$ in semiconductors, and 10 Å for metals. It is not clear at the present time whether the larger-than-expected magnitude of the observed mixing is due to an underestimated value of $\langle r^2 \rangle$ or to other contributory mechanisms. Further work is under way which examines the dependence of mixing on other parameters in order to clarify the origin of the observed effects.

In summary, we present a method that uses very thin markers in conjunction with backscattering spectrometry to investigate the intermixing of atoms induced by penetrating ions in a target. The feasibility of the method is established. Its advantages and drawbacks are discussed. Results are presented which show that the marker spreading varies as a function of depth within the range of the ion in the target. A preliminary interpretation of the results suggests that the amount of marker spreading correlates with the damage profile. The method holds much promise for experimentally studying ion-beam-induced solid interactions in detail.

The authors are grateful to J.W. Mayer, D.K. Brice, D.A. Thompson, and I. Golecki for their interest and helpful discussions. They also wish to thank J. Mallory for his skillful sample preparation, and the financial assistance provided by the Office of Naval Research (L.R. Cooper).

[1]See, for example, G. Carter and W.A. Grant in *Ion Implantation of Semiconductors*, (Edward Arnold Publisher, London, 1976), Chap. 5; J.W. Mayer, L. Eriksson, and J.A. Davies in *Ion Implantation in Semiconductors*, (Academic, New York, 1970), pp. 73–76 and references therein.
[2]See, for example, G. Dearnaley, J.H. Freeman, R.S. Nelson, and J. Stephen, in *Ion Implanation*, (North-Holland, New York, 1973), p. 137 and references therein.
[3]D.H. Lee, R.R. Hart, and O.J. Marsh, Appl. Phys. Lett. **20**, 73 (1972).
[4]R.R. Hart, D.H. Lee, and O.J. Marsh, Appl. Phys. Lett. **20**, 77 (1972).
[5]D.H. Lee, R.R. Hart, D.A. Kiewit, and O.J. Marsh, Phys. Status Solidi A **15**, 645 (1973).
[6]W.F. van der Weg, D. Sigurd, and J.W. Mayer in *Applications of Ion Beams to Metal*, edited by S.T. Picraux, E.D. EerNisse, and F.L. Vook (Plenum, New York, 1974), p. 209.
[7]J.M. Poate and T.C. Tisone, Appl. Phys. Lett. **24**, 391 (1974).
[8]B.Y. Tsaur, Z.L. Liau, and J.W. Mayer, Appl. Phys. Lett. **34**, 167 (1979).
[9]S. Matteson, J. Roth, and M-A. Nicolet, Radiat. Eff. (to be published).
[10]K.L. Wang, F. Bacon, and R.F. Reihl, J. Vac. Sci. Technol. **16**, 130 (1979).
[11]Z.L. Liau, J.W. Mayer, W.L. Brown, and J.M. Poate, J. Appl. Phys. **49**, 5295 (1978).
[12]P.K. Haff and Z.E. Switkowski, J. Appl. Phys. **48**, 3383 (1977).
[13]H.H. Andersen, Appl. Phys. **18**, 131 (1979).
[14]S. Matteson, G. Mezey, B.Y. Tsaur, and M-A. Nicolet (unpublished).
[15]K. Bruce Winterbon, in *Ion Implantation Range and Energy Deposition Distribution*, (Plenum, New York, 1975), Vol. 2.

ERRATA

Erratum: Efficient conversion of surface acoustic waves in shallow gratings to bulk plate modes [Appl. Phys. Lett. 34, 324 (1979)]

John Melngailis
Lincoln Laboratory, Massachusetts Institute of Technology, Lexington, Massachusetts 02173

H. A. Haus and A. Lattes
Massachusetts Institute of Technology, Research Laboratory of Electronics, Cambridge, Massachusetts 02139

PACS numbers: 31.50. + w, 31.70.Hq, 32.50. + d, 99.10. + g

In Equation 1, p mistakenly appears in place of d. It should read

$$k_w = [(\omega/c_s)^2 - (n\pi/d)^2]^{1/2} \quad \text{and} \quad k_w = [(\omega/c_c)^2 - (m\pi/d)^2]^{1/2},$$

where d is the thickness of the slab.

 0003-6951/79/220828-01$00.00